Surface and Electrostatic Contributions to DNA-Promoted Reactions of Platinum(II) Complexes with Short Oligonucleotides: A Kinetic Study

Sofi K. C. Elmroth

Inorganic Chemistry 1, Chemical Center, Lund University, P.O. Box 124, S-221 00 Lund, Sweden

Stephen J. Lippard*

Department of Chemistry, Massachusetts Institute of Technology, Cambridge, Massachusetts 02139

Received March 2, 1995[⊗]

The kinetics and mechanism for reactions of *cis*-$[Pt(NH_3)(NH_2C_6H_{11})Cl_2]$, **1**, and *cis*-$[Pt(NH_3)(NH_2C_6H_{11})Cl(OH_2)]^+$, **2a**, with phosphorothioate- and d(GpG)-containing oligodeoxyribonucleotides were investigated in phosphate-buffered aqueous solution at 25 °C. The rate of covalent adduct formation was studied as a function of pH, oligonucleotide length, and ionic strength. The results were consistent with a common mechanism in which **2a** serves as the active platinating reagent. The average rate constant for the acid hydrolysis of **1** was determined to be $(1.9 \pm 0.7) \times 10^{-5}$ s^{-1} from experiments with d(Tp(S)T) and $d(T_8p(S)T_8)$ as trapping reagents. The pK_a value of **2a** was determined to be 6.4 ± 0.2 from a series of its reactions with $d(T_8p(S)T_8)$ at $[Na^+] = 0.064$ M and $5.80 \leq pH \leq 8.00$. Direct platination of oligonucleotides with **2a** at both phosphorothioate sites and d(GpG) sequences exhibited a similar length dependence, with up to a 40-fold rate increase as the DNA lengthened from 2 to 16 nucleotides at $[Na^+] = 0.064$ M. The apparent second-order rate constants for platination with **2a** at $[Na^+] = 0.064$ M and 25 °C were 0.080 ± 0.016 M^{-1} s^{-1} for d(Tp(S)T), 1.64 ± 0.11 M^{-1} s^{-1} for $d(T_4p(S)T_4)$, 3.1 ± 0.4 M^{-1} s^{-1} for $d(T_8p(S)T_8)$, 0.026 ± 0.004 M^{-1} s^{-1} for d(GpG), and 0.92 ± 0.04 M^{-1} s^{-1} for $d(T_7GGT_7)$. The rate constants of phosphorothiote adduct formation were the same for both single- and double-stranded oligonucleotides. The apparent second-order rate constants for disappearance of unplatinated oligonucleotides were 0.56 ± 0.09 M^{-1} s^{-1} for $d(T_8p(S)T_8)$ and 0.56 ± 0.08 M^{-1} s^{-1} for $d(T_8p(S)T_8)$•$d(A_{16})$, at $[Na^+] = 0.064$ M and 0 °C. The influence of sodium ion concentration on the rate of adduct formation, with $NaClO_4$ as supporting electrolyte, was probed by studying the reaction of **2a** with $d(T_np(S)T_n)$, where $n = 1$, 4, or 8. The apparent second-order rate constants for platination of the two longer oligonucleotides decreased as a function of increasing ionic strength and exhibited a similar reactivity at $[Na^+] = 0.772$ M. Apparent second-order rate constants for platination with **2a** at 25 °C were 0.624 ± 0.007 M^{-1} s^{-1} for $d(T_4p(S)T_4)$ and 0.58 ± 0.06 M^{-1} s^{-1} for $d(T_8p(S)T_8)$. The reactivity of d(Tp(S)T) increased slightly in the same $[Na^+]$ interval but remained below that of the longer oligonucleotides even at high ionic strength. The apparent rate constant for platination with **2a** was $k_{2,app} = 0.230 \pm 0.032$ M^{-1} s^{-1} at $[Na^+] = 0.772$ M and 25 °C. The variations in reactivity with oligonucleotide length cannot be explained solely on the basis of a mechanism involving nonselective cation condensation which results in local increases of the concentration of **2a** on the polymer. A significant pathway for the reaction mechanism is postulated to involve directed diffusion along the DNA, similar to that suggested for protein target location.

Introduction

Knowledge of the principles governing interactions between metal ions and nucleic acids is important for understanding both the structural and dynamic features of the biopolymer itself,[1−7] as well as its interactions with other molecules.[8−13] The polyelectrolyte theory has proved to be a useful tool for describing phenomena arising mainly from weak electrostatic interactions between the negatively charged polymer phosphate backbone and ions in its vicinity.[14−16] For covalent modification of DNA, experimental information about parameters that influence the reactivity is scarce.[17−24]

[⊗] Abstract published in *Advance ACS Abstracts,* September 1, 1995.

(1) Saenger, W. *Principles of Nucleic Acid Structure*; Springer-Verlag: New York, 1988.
(2) Leng, M. *Biophys. Chem.* **1990**, *35*, 155−163.
(3) Pyle, A. M.; Barton, J. K. *Prog. Inorg. Chem.* **1990**, *38*, 413−475.
(4) Sundquist, W. I.; Lippard, S. J. *Coord. Chem. Rev.* **1990**, *100*, 293−322.
(5) Pyle, A. M. *Science* **1993**, *261*, 709−714.
(6) Sigel, H. *Chem. Soc. Rev.* **1993**, *22*, 255−267.
(7) Black, C. B.; Huang, H.-W.; Cowan, J. A. *Coord. Chem. Rev.* **1994**, *135−136*, 165−202.
(8) Bruhn, S. L.; Toney, J. H.; Lippard, S. J. *Prog. Inorg. Chem.* **1990**, *38*, 477−516.
(9) Record, M. T.; Ha, J.-H.; Fisher, M. A. *Methods Enzymol.* **1991**, *208*, 291−343.
(10) Lohman, T. M.; Mascotti, D. P. *Methods Enzymol.* **1992**, *212*, 400−424.
(11) Comess, K. M.; Lippard, S. J. In *Mol. Aspects Anticancer Drug-DNA Interact.* **1993**, 134−168.
(12) Chu, G. *J. Biol. Chem.* **1994**, *269*, 787−790.
(13) Papavassiliou, A. G. *Biochem. J.* **1995**, *305*, 345−357.
(14) Manning, G. S. *Q. Rev. Biophys.* **1978**, *2*, 179−246.
(15) Anderson, C. F.; Record, M. T. *Annu. Rev. Biophys. Biophys. Chem.* **1990**, *19*, 423−465.
(16) Olmsted, M. C.; Bond, J. P.; Anderson, C. F.; Record, M. T. *Biophys. J.* **1995**, *68*, 634−647.
(17) Sundquist, W. I.; Bancroft, D. P.; Chassot, L.; Lippard, S. J. *J. Am. Chem. Soc.* **1988**, *110*, 8559−8560.
(18) Malinge, J.-M.; Sip, M.; Blacker, A. J.; Lehn, J.-M.; Leng, M. *Nucleic Acids Res.* **1990**, *18*, 3887−3891.
(19) Bernges, F.; Holler, E. *Eur. J. Biochem.* **1992**, *208*, 573−579.
(20) Kierzek, R. *Nucleic Acids Res.* **1992**, *20*, 5073−5077.
(21) Reedijk, J. *Inorg. Chem. Acta* **1992**, *198−200*, 873−881.

0020-1669/95/1334-5234$09.00/0

One of the better investigated chemical reactions is the covalent adduct formation by the anticancer drug cisplatin, *cis*-$[Pt(NH_3)_2Cl_2]$,[25,26] and related compounds with synthetic and natural DNAs. The commonly accepted DNA-binding mechanism for cisplatin in vivo involves formation of the aqua complex *cis*-$[Pt(NH_3)_2Cl(OH_2)]^+$.[8,26,27] Subsequent nucleophilic attack by purine N7 atoms is rapid compared to the initial loss of chloride ion from the coordination sphere.[8,21,26-28] The sequence selectivity and rate of this DNA platination step depend on the nature of both the target DNA and the platinum complex. Factors such as the local accumulation of cations on the polymer, orientational effects, facilitated diffusion, and linkage isomerization reactions influence both the reactivity and the final location of the metal complex,[17-19,27,29-35] but a detailed mechanistic interpretation has not yet been presented. In particular, the effects of electrostatic and surface interactions with the polymer prior to covalent bond formation have not been systematically investigated.

Recently we reported preliminary observations which revealed that the rate of covalent adduct formation between a cationic Pt(II) reagent and short oligonucleotides depends on the polymer length.[24] The present investigation is an extension of that work and was carried out to provide a more detailed description of the mechanism of platination. An effort was made to separate contributions from nonspecific accumulation of cations on the DNA surface, the local concentration effect, from factors that influence covalent adduct formation. In particular, we studied DNA platination by two metabolites of the recently developed and orally administered anticancer drug *cis,trans,cis*-ammine(cyclohexylamine)bis(butyrato)dichloroplatinum(IV),[36] namely, *cis*-$[Pt(NH_3)(NH_2C_6H_{11})Cl_2]$ (**1**) and *cis*-$[Pt(NH_3)NH_2C_6H_{11})Cl(OH_2)]^+$ (**2a**), Chart 1, with oligo(dT) fragments containing a phosphorothioate or embedded d(GpG) sequence. These platinum metabolites are structurally related to cisplatin and its first hydrolysis product. Examination of their adduct profiles on DNA revealed, as in the case of cisplatin, a strong preference to form intrastrand d(GpG) cross-links.[37,38] We used these complexes rather than cisplatin to obtain the kinetic profiles for DNA binding because their DNA adducts are better resolved by the HPLC methodology employed. A single phosphorothioate linkage or d(GpG) sequence was introduced in the middle of each oligonucleotide to ensure adduct regiospecificity,[39-43] which facilitated the interpretation of the kinetics data.

Chart 1

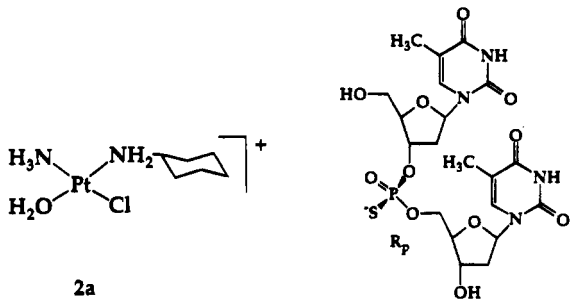

Experimental Section

Chemicals and Reagents. The synthesis of *cis*-$[Pt(NH_3)(NH_2C_6H_{11})Cl_2]$, **1**, has been described previously.[37] Solutions of cis-$[Pt(NH_3)(NH_2C_6H_{11})Cl(OH_2)]^+$, **2a**, were prepared by addition of 0.98 equiv of $AgNO_3$ (Mallinckrodt) to a solution of **1** dissolved in DMF (Fisher). A solution of *cis*-$[Pt(NH_3)_2Cl(OH_2)]^+$, **4a**, in DMF was prepared similarly from *cis*-$[Pt(NH_3)_2Cl_2]$ (Johnson Matthey), **3**. The reaction mixtures were allowed to vortex in the dark for ca. 14 h prior to removal of the precipitated AgCl by centrifugation. Stock solutions of **2a** and **4a** in DMF were stored at 4 °C. Chloro(2,2′:6′,2″-terpyridine)-platinum(II), **5**, was prepared as previously described.[44] Stock solutions of **5** in 0.10 M NaCl(aq) (Sigma) were stored at room temperature. Buffers, $5.80 \leq pH \leq 8.00$ and $[P_i] = 0.050$ M, were prepared from aqueous stock solutions of 0.10 M NaH_2PO_4 (Sigma) and 0.10 M NaOH (Mallinckrodt) according to standard procedures.[45] Doubly distilled, deionized water was used to prepare all aqueous solutions. The oligonucleotides d(Tp(S)T), Chart 1, $d(T_8p(S)T_8)$, $d(T_4p(S)T_4)$, d(GpG), $d(t_7GGT_7)$, and $d(A_{16})$ were synthesized by standard phosphoramidite methodology[46] and purified by size exclusion chromatography (G-25 Sephadex, Pharmacia). When impurities from shorter fragments were detected by high-performance liquid chromatography (HPLC), the oligonucleotides were further purified by reverse-phase HPLC. Stock solutions of oligonucleotides and lyophilized DNA powders were stored at −20 °C.

HPLC Measurements. Chromatograms were obtained by use of a Perkin-Elmer Series 4 liquid chromatograph linked to a LC 95 UV/vis detector set to 260 nm and a LCI-100 integrator. Separation of platinated oligonucleotides from the unplatinated starting material was achieved under reverse-phase conditions with a Vydac protein and peptide C18 column equipped with a guard. Solutions of 0.10 M NH_4OAc (Mallinckrodt, analytical reagent) adjusted to pH 6.0 with HOAc (Mallinckrodt, Analytical Reagent), **A**, and a 1:1 mixture of 0.10 M NH_4OAc, pH 6.0, and CH_3CN (Fisher, HPLC grade), **B**, were used as eluants. Typically, linear gradients in which the ratio A:B changed from 95:5 to 40:60 over 30 min (dinucleotides) or from 85:15 to 40:60 over 30 min (hexadecanucleotides) were used to resolve the eluted peaks.

Spectrophotometric Measurements. UV/visible spectra were recorded on a Perkin-Elmer Lambda 7 or a HP-8452a diode array

(22) Hänsler, U.; Rokita, S. E. *J. Am. Chem. Soc.* **1993**, *115*, 8554−8557.
(23) Zou, Y.; Van Houten, B.; Farrell, N. *Biochemistry* **1993**, *32*, 9632−9638.
(24) Elmroth, S. K. C.; Lippard, S. J. *J. Am. Chem. Soc.* **1994**, *116*, 3633−3634.
(25) Loehrer, P. J.; Einhorn, L. H. *Ann. Intern. Med.* **1984**, *100*, 704−713.
(26) Green, M.; Garner, M.; Orton, D. M. *Transition Met. Chem.* **1992**, *17*, 164−176.
(27) Bancroft, D. P.; Lepre, C. A.; Lippard, S. J. *J. Am. Chem. Soc.* **1990**, *112*, 6860−6871.
(28) Arpalahti, J.; Mikola, M.; Mauristo, S. *Inorg. Chem.* **1993**, *32*, 3327−3332.
(29) Malinge, J.-M.; Leng, M. *Proc. Natl. Acad. Sci. U.S.A.* **1986**, *83*, 6317−6321.
(30) Comess, K. M.; Costello, C. E.; Lippard, S. *J. Biochemistry* **1990**, *29*, 2102−2110.
(31) Gaucheron, F.; Malinge, J.-M.; Blacker, A. J.; Lehn, J.-M.; Leng, M. *Proc. Natl. Acad. Sci. U.S.A.* **1991**, *88*, 3516−3519.
(32) Anin, M.-F.; Gaucheron, F.; Leng. M. *Nucleic Acids Res.* **1992**, *20*, 4825−4830.
(33) Gonnet, F.; Kozelka, J.; Chottard, J.-C. *Angew. Chem., Int. Ed. Engl.* **1992**, *31*, 1483−1485.
(34) Ren, T.; Bancroft, D. P.; Sundquist, W. I.; Masschelein, A.; Keck, M. V.; Lippard, S. J. *J. Am. Chem. Soc.* **1993**, *115*, 11341−11352.
(35) Dalbiès, R.; Payet, D.; Leng, M. *Proc. Natl. Acad. Sci. U.S.A.* **1994**, *91*, 8147−8151.
(36) Kelland, L. R.; Murrer, B. A.; Abel, G.; Giandomenico, C. M.; Mistry, P.; Harrap, K. R. *Cancer Res.* **1992**, *52*, 822−828.
(37) Hartwig, J. F.; Lippard, S. J. *J. Am. Chem. Soc.* **1992**, *114*, 5646−5654.
(38) Yarema, K. J.; Wilson, J. M.; Lippard, S. J.; Essigmann, J. M. *J. Mol. Biol.* **1994**, *236*, 1034−1048.
(39) Szalda, D. J.; Eckstein, F.; Sternbach, H.; Lippard, S. J. *J. Inorg. Biochem.* **1979**, *11*, 279−282.
(40) Fichtinger-Schepman, A. M. J.; van der Veer, J. L.; den Hartog, J. H. J.; Lohman, P. H. M.; Reedijk, J. *Biochemistry* **1985**, *24*, 707−713.
(41) Chu, B. C. F.; Orgel, L. E. *Nucleic Acids Res.* **1990**, *18*, 5163−5171.
(42) Gruff, E. S.; Orgel, L. E. *Nucleic Acids Res.* **1991**, *19*, 6849−6854.
(43) Chu, B. C. F.; Orgel, L. E. *Nucleic Acids Res.* **1992**, *20*, 2497−2502.
(44) Howe-Grant, M.; Lippard, S. J. *Inorg. Synth.* **1980**, *20*, 101−105.
(45) *Handbook of Chemistry and Physics*; CRC Press: Boca Raton, FL, 1979−1980; p D−148.
(46) Zon, G.; Stec, W. J. In *Oligonucleotids and Analogues—A Practical Approach*; Eckstein, F., Ed.; Oxford University Press: New York, 1991; pp 87−108.

Table 1. ^{31}P and ^{195}Pt Chemical Shifts for Oligonucleotide Phosphorothioates and Selected Platinum Adducts

species	$\delta(^{31}P)$, ppm[a,b]	solvent
d(Tp(S)T)	54.6(S_p), 54.9(R_p)[c]	H_2O
$d(T_8p(S)T_8)$	54.1(S_p), 54.3(R_p)[c]	buffer[d]
cis-$[Pt(NH_3)_2X]$-$d(T_8p(S)T_8)^m$ X = OH_2 ($m = 13-$); OH^- ($m = 14-$); Cl^- ($m = 14-$)	37.4−38.5, multiplet	buffer[d]
cis-$[Pt(NH_3)(NH_2C_6H_{11})X]$-$d(Tp(S)T)^m$ X = OH_2 (m = 1+); OH^- (m = 0); Cl^- ($m = 0$)	37.3−38.5, multiplet	H_2O
$[Pt(terpy)]$-d(Tp(S)T)$^+$	32.6, 35.6[e]	H_2O

[a] Relative to external H_3PO_4 at 0 ppm. S_p and R_p refer to the phosphorothioate diastereomers. [b] Spectra are reported in Figures 1 and S2 (Supporting Information). [c] Assignments were made according to ref 47. [d] 50 mM NaH_2PO_4, pH 6.50. [e] $\delta(^{195}Pt) = -2962$ and -2978 ppm; external K_2PtCl_4 at -1624 ppm used as reference.

spectrophotometer. Concentrations of the oligonucleotide stock solutions were determined at ambient temperature from their absorbance at 260 nm. The introduction of a single phosphorothioate linkage was assumed to have a negligible contribution to the overall absorbance.

NMR Spectroscopy. ^{31}P and ^{195}Pt NMR spectra were obtained on a Varian XL 300 MHz instrument. The chemical shifts for the ^{31}P NMR spectra were referenced to external 30% H_3PO_4 (Mallinckrodt, Analytical Reagent) in D_2O, which was used as internal lock. The chemical shifts for ^{195}Pt NMR spectra are reported relative to K_2PtCl_6 and were referenced externally to K_2PtCl_4.

Kinetics Studies. The kinetics of reactions between **1** or **2a** and the single-stranded oligonucleotides were followed at 25 °C and pH 6.50, $[P_i] = 0.050$ M. Comparison of the reactivity of **2a** with single- and double-stranded oligonucleotides was performed at 0 °C to maximize duplex stability (T_m for the duplex was determined as ca. 28 °C, Figure S1 (Supporting Information)). Reactions were initiated by addition of a small volume of a concentrated solution of Pt(II) in DMF to a temperature-equilibrated and buffered oligonucleotide solution. Aliquots of the reaction mixtures were removed at appropriate time intervals and quenched immediately with a 5−10-fold excess of buffer. The samples were frozen and stored at −196 °C. Analyses were made within 30 h from freezing. The relative changes in the combined reactant or product HPLC peak areas were used to monitor the course of the reactions.

Results

NMR Spectroscopic Characterization of Platinum−Phosphorothioate Adducts. The reactions between each of the platinum complexes **2a**, **4a**, and **5** and phosphorothioate-containing oligonucleotides d(Tp(S)T) and $d(T_8p(S)T_8)$ were followed qualitatively by ^{31}P and ^{195}Pt NMR spectroscopy. The NMR spectra were recorded at ambient temperature, and typical reaction conditions were [Pt(II)]:[oligonucleotide) ≈ 1:1, with total concentrations of each reagent in the range 5−10 mM. The rate of adduct formation was too rapid to be evaluated by the NMR technique under these conditions, with conversion to products within less than 30 min. Initial product spectra were recorded within ca. 2 h from mixing. No changes in the product peak position or in the relative intensity of the signals were observed even after prolonged storage of the reaction mixtures, 2−6 months, at room temperature. ^{31}P and ^{195}Pt chemical shifts are summarized in Table 1. The ^{31}P NMR spectrum of a mixture of the two R_p and S_p phosphorothioate diastereomers contained two signals at ca. 54 ppm for both d(Tp(S)T) and $d(T_8p(S)T_8)$. Addition of the monofunctional complex **5** converted these signals to two new ones at 32.6 and 35.6 ppm, which we attribute to Pt−S bond formation (Figure 1a). This conclusion was further supported by the appearance of two separate ^{195}Pt NMR signals at −2962 and −2978 ppm (Figure 1b). Reactions of the bifunctional complexes **2a** and **4a** with the diastereomeric mixture of $d(T_np(S)T_n)$ similarly gave rise

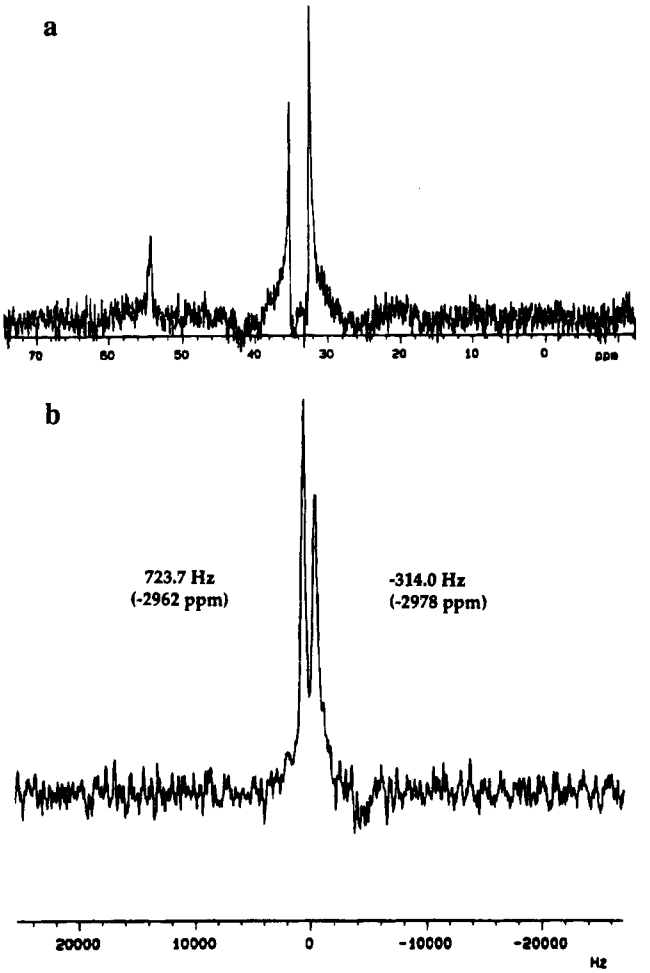

Figure 1. (a) ^{31}P NMR spectrum of a reaction mixture of d(Tp(S)T), 6.3 mM, and $[Pt(terpy)Cl]^+$, 5.4 mM, in H_2O. Resonances from unplatinated d(Tp(S)T) can be seen at ca. 55 ppm, and the resonances from Pt adducts of the two diastereomers of the oligonucleotide, at ca. 32 and 36 ppm. (b) ^{195}Pt NMR spectrum of the reaction mixture in (a) recorded with a transmitter frequency of 64.287 MHz. K_2PtCl_4, at 64.374 MHz (−1624 ppm), was used as an external reference.

to upfield shifts in the phosphorothioate ^{31}P NMR signals by ca. 15−17 ppm compared to their position in the unplatinated oligonucleotides (Figure S2). The multiple signals observed after addition of **2a** to d(Tp(S)T) and after addition of **4a** to $d(T_8p(S)T_8)$ arose from the presence of several platinum adducts of the type $[Pt(NH_3)(NH_2R)d(T_np(S)T_n)X]^{3-2n}$, where X = OH_2, OH^- or Cl^-, at thermodynamic equilibrium.

Kinetic Studies. Product Distribution and Data Analysis. The kinetics for reactions between $d(T_np(S)T_n)$, $n = 1$, 4, 8, and compound **2a** were evaluated by the time-dependent changes in integrated HPLC areas for both unplatinated and platinated oligonucleotides. The sum of peak areas corresponding to the unplatinated oligonucleotides, both R_p and S_p diastereomers,[47] as well as those corresponding to the products, exhibited exponential time-dependent behavior under pseudo-first-order conditions with Pt(II) in excess. Sample HPLC traces for the reaction of d(Tp(S)T) with **2a** are given in Figure 2. The time dependence was characterized by decay of peaks corresponding to the unplatinated diastereomers, which eluted with a retention time, t_r, in the region 19−23 min, and a parallel buildup of a major initial product peak eluting at $t_r \approx 39$ min. As indicated by the last two traces in Figure 2, after the disappearance of unplatinated oligonucleotides there was product redistribution leading to formation of an additional peak migrating with $t_r \approx$

(47) Eckstein, F. *Angew. Chem., Int. Ed. Engl.* **1983**, *22*, 423−439.

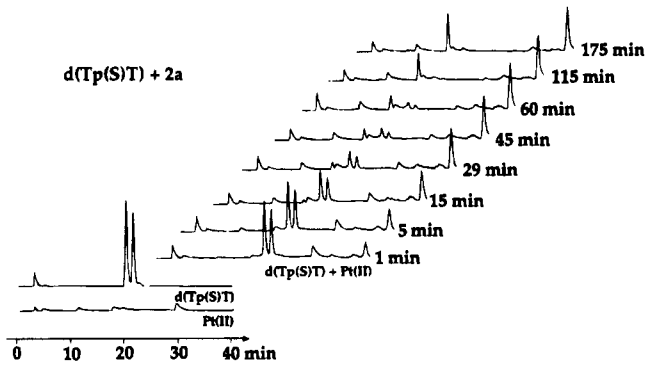

Figure 2. Representative HPLC traces for the reaction of **2a** with d(Tp(S)T), [Pt(II)] = 4.98 × 10^{-3} M, [d(Tp(S)T] = 9.53 × 10^{-5} M, I = 0.078 M, pH 6.50, T = 25.0 °C.

16 min, close to that of the unplatinated phosphorothioates. The time course for this redistribution was similar to that observed for **2a** alone which, at 25 °C and pH 6.50, converted from a major peak eluting at ≈30 min to one with $t_r \approx 12$ min over a period of 1−2 h. The peak observed at short retention time in all HPLC traces, $t_r \approx 3$ min, was due to the absorbance of coinjected phosphate buffer.

The reaction of **2a** with d(T_4p(S)T_4) and d(T_8p(S)T_8) was studied in a similar fashion. The two unplatinated oligonucleotide diastereomers had retention times of ca. 17−19 min, and at least four different product peaks, with varying relative ratios, could be identified at $t_r \approx 19$−25 min (Figures S3 and S4 (Supporting Information)). The sum of the integrated HPLC areas in each region was used to determine the pseudo-first-order rate constant for both disappearance of reactants, k_{react}, and appearance of products, k_{prod}. The observed rate constant, k_{obsd}, was determined as the average of k_{react} and k_{prod} unless stated otherwise. The non-zero residual peak area for the reactants d(T_4p(S)T_4) and d(T_8p(S)T_8) at the end of the initial phase was interpreted as the result of decreasing resolution between peaks corresponding to products with short retention times and those of the unplatinated ones (cf. Figure 2). Control experiments were also performed with **2a** and $(dT)_{16}$ as reactants. In the absence of the specific binding sites, phosphorothioate or d(GpG), no changes in the area or retention time of the peaks corresponding to the reactants were observed.

Reaction Order. The rate equations for the reaction of **2a** with d(T_np(S)T_n), where n = 1, 4, or 8, were determined under pseudo-first-order conditions with **2a** in excess. The kinetics followed first-order behavior and were fit to a single-exponential function (Figure S3 (Supporting Information)). The concentration of the excess reagent was varied at [Na^+] = 0.064 M and 25 °C (experimental conditions are given in Table S1 (Supporting Information)). A plot of the observed pseudo-first-order rate constants as a function of the total concentration of added **2a**, [Pt(II)], is given in Figure 3. The linear dependence and effectively zero intercept indicate the rate law for adduct formation given in eq 1. The corresponding relation between

$$\frac{-\mathrm{d}[\mathrm{d}(T_n\mathrm{p(S)}T_n)]}{\mathrm{dt}} = \frac{\mathrm{d[prod]}}{\mathrm{dt}} = k_{2,\mathrm{app}}[\mathrm{Pt(II)}][\mathrm{d}(T_n\mathrm{p(S)}T_n)] \quad (1)$$

$$k_{\mathrm{obsd}} = k_{2,\mathrm{app}}[\mathrm{Pt(II)}] \quad (2)$$

the observed rate constant, k_{obsd}, and the apparent second-order one, $k_{2,app}$, is given by eq 2. The $k_{2,app}$ values, determined by using eqs 1 and 2, were 0.080 ± 0.016 M^{-1} s^{-1} for d(Tp(S)T), 1.64 ± 0.11 M^{-1} s^{-1} for d(T_4p(S)T_4), and 3.1 ± 0.4 M^{-1} s^{-1} for d(T_8p(S)T_8) at pH 6.50. The magnitudes of these apparent second-order rate constants depend almost linearly on the length of the target oligonucleotide fragments, with an approximate 40-fold rate increase for adduct formation on d(T_8p(S)T_8) compared to d(Tp(S)T) (Table 2 and Figure S5 (Supporting Information)). The rate of adduct formation was also followed at 0 °C for both single-stranded and double-stranded DNA. Pseudo-first-order kinetics was observed for the disappearance of unplatinated oligonucleotides for both these DNAs (Figure 4). The overall rates of platination with **2a** were similar for d(T_8p(S)T_8) and d(T_8p(S)T_8)·d(A_{16}) at 0 °C, with apparent second-order rate constants 0.56 ± 0.09 and 0.55 ± 0.08 M^{-1} s^{-1}, respectively. Control experiments with [d(T_np(S)T_n)] in excess over [Pt(II)] were also carried out and revealed a reactivity in agreement with the rate law given in eq 1 under these conditions (data not shown).

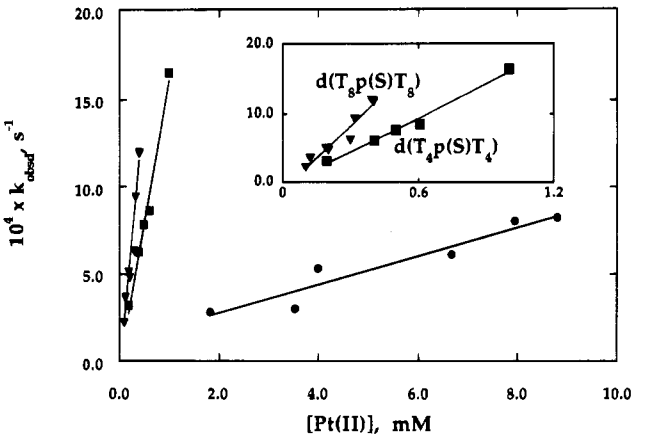

Figure 3. Observed pseudo-first-order rate constants as a function of total concentration, [Pt(II)], for the reaction of **2a** with d(Tp(S)T) (circles), d(T_4p(S)T_4) (squares), and d(T_8p(S)T_8) (triangles) as a function of the concentration of [Pt(II)]. The insert shows an enlargement of the region 0 < [Pt(II)] < 1.2 mM.

Table 2. Summary of Apparent Second-Order Rate Constants Obtained for Specific Platination of Phosphorothioate- and Guanosine-Containing Oligonucleotides[a]

oligonucleotide	$k_{2,app}$, M^{-1} s^{-1}	[Na^+], M	relative reactivity
d(GpG)	0.026 ± 0.004	0.064	0.33
d(Tp(S)T)	0.080 ± 0.016	0.064	1.0
	0.101 ± 0.014	0.114	1.3
	0.164 ± 0.010	0.164	2.2
	0.183 ± 0.013	0.264	3.5
	0.142 ± 0.048	0.386	1.8
	0.230 ± 0.032	0.772	2.9
d(T_4p(S)T_4)	1.64 ± 0.11	0.064	20
	0.624 ± 0.007	0.772	7.8
d(T_7GGT_7)	0.92 ± 0.04	0.064	11
d(T_8p(S)T_8)	3.1 ± 0.4	0.064	39
	1.72 ± 0.03	0.114	21
	1.35 ± 0.07	0.164	17
	0.87 ± 0.32	0.214	11
	0.59 ± 0.09	0.464	7.4
	0.58 ± 0.06	0.772	7.2
	0.73 ± 0.04	0.964	9.1

[a] 25 °C, pH 6.50, [P_i] = 5.00 × 10^{-2} M. The ionic strength was adjusted with $NaClO_4$. Observed pseudo-first-order rate constants are reported in Tables S1 and S2 (Supporting Information).

Influence of Target Site on Reactivity. The influence of the specific target on the apparent second-order rate constants was investigated by comparing the reactivity of the phosphorothioate sites with that of d(GpG) sequences in oligonucleotide fragments of the same total length. Complex **2a** was used as the platination reagent, and the experiments were performed at pH 6.50 and 25 °C under pseudo-first-order conditions with

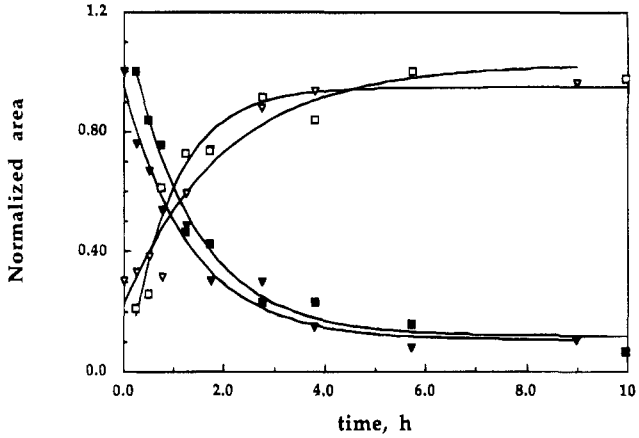

Figure 4. Experimental data points and theoretical fits to a single-exponential function for platination by **2a** of single-stranded (triangles) and double-stranded (squares) DNA. Filled symbols refer to loss of starting material, and open symbols, to product formation. The experiments were performed at 0 °C, pH 6.50, and with [Pt(II)] = 3.74×10^{-4} M, [d(T_8p(S)T_8)] = 1.0×10^{-5} M (single-stranded) and [Pt(II)] = 3.80×10^{-4} M, [d(T_8p(S)T_8] = 1.0×10^{-5} M.

[Pt(II)] in excess. Two examples of the time-dependent changes in the integrated HPLC areas for the unplatinated oligonucleotides are given in Figure 5a,b. The kinetic traces indicated that the phosphorothioate sites in both d(Tp(S)T) and d(T_8p(S)T_8) were more reactive than the d(GpG) and d(T_7GGT_7) sequences under similar conditions. Evaluation of the apparent second-order rate constants according to eq 2 revealed that platination of the phoshorothioate site was ca. 3 times faster than formation of the monofunctional d(GpG) adduct on both the dimers and the hexadecanucleotides. The corresponding rate acceleration caused by increasing the length of the oligonucleotide is a factor of ca. 35 for the d(GpG) sequence and of ca. 39 for the phosphorothioate site (see also Table 2).

pH Dependence. The pH dependence of the reaction between *cis*-[Pt(NH_3)($NH_2C_6H_{11}$)(OH_2)]$^+$, **2a**, and d(T_8p(S)T_8) was investigated in the interval 5.80 ≤ pH ≤ 8.00. A summary of experimental conditions and observed pseudo-first-order rate constants is given in Table 3 (see also Figure S6 (Supporting Information)). The decrease in reactivity observed as a function of increasing pH was interpreted to reflect an increasing concentration of the relatively unreactive monohydroxo species[48-50] *cis*-[Pt(NH_3)($NH_2C_6H_{11}$)Cl(OH)], **2b**. The experimental data were fit to a theoretical expression by assuming a rapid, pH dependent preequilibrium between **2a** and **2b**, eq 3, followed

$$\mathbf{2a} \overset{K_a}{\rightleftharpoons} \mathbf{2b} + H^+ \quad (3)$$

$$\mathbf{2a} + d(T_8p(S)T_8) \xrightarrow{k_2'} \text{product} \quad (4)$$

by a rate-determining second-order reaction between **2a** and the oligonucleotide, eq 4.[27,28] The resulting expression for the observed pseudo-first-order rate constant under conditions with [**2a**] ≫ [d(T_8p(S)T_8] is given by eq 5, where [Pt(II)] = [**2a**] + [**2b**]. The expression for the apparent second-order rate constant is given by eq 6. The equilibrium constant K_a was determined to be $(4.1 \pm 1.9) \times 10^{-7}$ M, pK_a = 6.4 ± 0.2. The observed pseudo-first-order rate constant in acidic solution was k_2'[Pt(II)] = $(1.34 \pm 0.22) \times 10^{-3}$ s^{-1}, corresponding to $k_2' = 7.1 \pm 1.1$ M^{-1} s^{-1}.

$$k_{obsd} = k_2' \frac{[H^+]}{[H^+] + K_a} [Pt(II)] \quad (5)$$

$$k_{2,app} = k_2' \frac{[H^+]}{[H^+] + K_a} \quad (6)$$

Acid Hydrolysis Pathway: Reaction of 1 with d(T_np(S)T_n). The reaction between **1** and either d(Tp(S)T) or d(T_8p(S)T_8) was studied by addition of a slight excess of the platinum compound to a solution of the oligonucleotide at pH = 6.50 and 25 °C. Introduction of a hydrolysis step (eq 7) was required to account for the induction period observed early in the course of the reaction (Figure 6), and adduct formation between d(T_np(S)T_n) and **1** was assumed to take place according to the mechanism defined by eqs 3, 7, and 8. The rate constant for

$$\mathbf{1} \xrightarrow{k_{ah}} \mathbf{2a} + Cl^- \quad (7)$$

$$\mathbf{2a} + d(T_np(S)T_n) \xrightarrow{k_2} \text{Pt–S adduct} \quad (8)$$

acid hydrolysis of **1**, k_{ah}, determined by FACSIMILE fitting[51] of the experimental data to this mechanism, was $(2.6 \pm 1.1) \times 10^{-5}$ s^{-1} for d(Tp(S)T) and $(1.26 \pm 0.54) \times 10^{-5}$ s^{-1} for d(T_8p(S)T_8). The rate constant was evaluated from three individual experiments with each oligonucleotide. A summary of the results and parameters used during the fitting procedure is given in Table 4. Examples of kinetic traces and simulated curves are provided in Figure 6.

Sodium Ion Dependence. The ionic strength dependence of the reactions of **2a** with the three oligonucleotides, d(T_np(S)T_n) (n = 1, 4, 8), was investigated in the interval 0.064 M ≤ [Na^+] ≤ 0.96 M. The apparent second-order rate constants for product formation were determined by assuming a linear dependence on the concentration of excess reagent and of the observed pseudo-first-order rate constant, according to eq 2. Figure 7 compares the apparent second-order rate constants for reactions involving d(Tp(S)T) and d(T_8p(S)T_8) as well as two control points for d(T_4p(S)T_4). Experimental details are given in Table S2 (Supporting Information), and examples of kinetic traces for reaction of **2a** with d(T_4p(S)T_4) and d(T_8p(S)T_8) at [Na^+] = 0.772 M under comparable reaction conditions are presented in Figure S7 (Supporting Information). The derived rate constants are summarized in Table 2.

Competition Experiments. The difference in reactivity between the reference system, d(Tp(S)T), and d(T_8p(S)T_8) was also investigated qualitatively with both DNA molecules present in solution. The reactions were studied under pseudo-first-order conditions with **2a** in excess, and the effective concentrations of phosphodiester linkages were similar for both reagents, that is, approximately a 10-fold excess of d(Tp(S)T) over d(T_8p(S)T_8). The results showed that platination of d(T_8p(S)T_8) occurs more rapidly in a situation with the competing reagent in large molar excess compared to the concentration of target on the longer DNA molecule. This phenomenon was most pronounced at [Na^+] = 0.064 M (Figure 8), where the peak-height of d(Ts(S)T) was not changed significantly during the first half-life of platination of d(T_8p(S)T_8). This behavior persisted even at [Na^+] = 0.772 M, where the first half-life of the d(T_8p(S)T_8) reaction could be estimated from peak heights to be ca. 30 min

(48) Arpalahti, J.; Lehikoinen, P. *Inorg. Chem.* **1990**, *29*, 2564–2567.
(49) Jacobs, R.; Prinsloo, F.; Breet, E. *J. Chem. Soc., Chem. Commun.* **1992**, 212–213.
(50) Berners-Price, S. J.; Frenkiel, T. A.; Frey, U.; Ranford, J. D.; Sadler, P. J. *J. Chem. Soc., Chem. Commun.* **1992**, 789–791.
(51) Curtis, A. R.; Sweetenham, W. P. *FACSIMILE/CHECKMAT User's Manual*; Harwell Laboratory: Harwell, U.K., 1988.

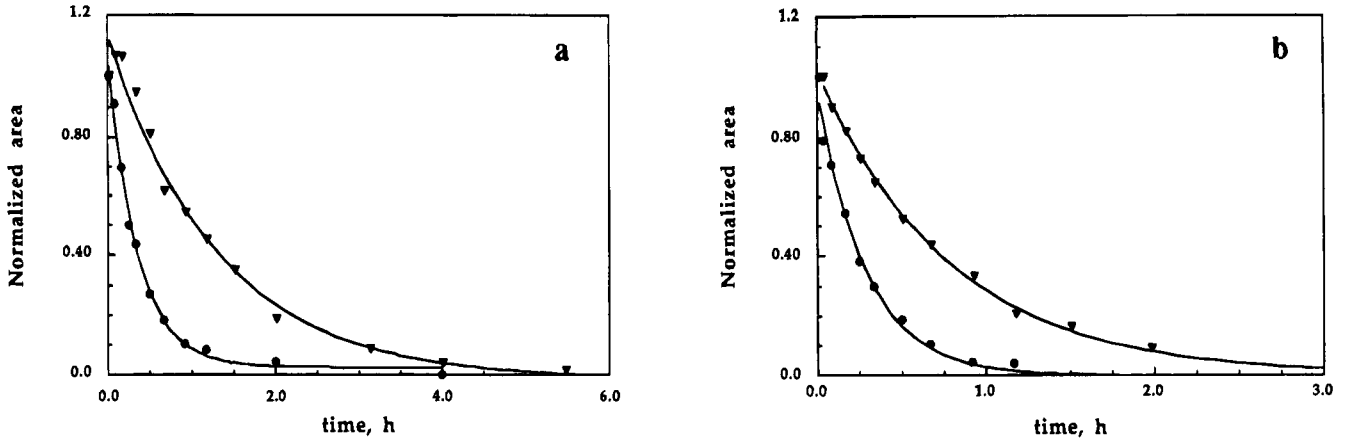

Figure 5. Experimental data points and fits to a single-exponential curve for the platination of (a) d(Tp(S)T) (circles), [Pt(II)] = 7.95×10^{-3} M, [d(Tp(S)T)] = 1.15×10^{-4} M, and d(GpG) (triangles), [Pt(II)] = 7.93×10^{-3} M, [d(GpG)] = 1.13×10^{-4} M, and (b) $d(T_8p(S)T_8)$ (circles), [Pt(II)] = 3.93×10^{-4} M, $[d(T_8p(S)_8T)] = 9.59 \times 10^{-6}$ M, and $d(T_7GGT_7)$ (triangles), [Pt(II)] = 3.93×10^{-4} M, $[d(T_7GGT_7)] = 9.82 \times 10^{-6}$ M.

Table 3. Observed Pseudo-First-Order Rate Constants for the Reaction of *cis*-$[Pt(NH_3)(NH_2C_6H_{11})Cl(OH_2)]^+$ with $d(T_8p(S)T_8)$ as a Function of pH[a]

pH	10^4k_{react}, s^{-1}	10^4k_{prod}, s^{-1}	10^4k_{obsd}, s^{-1}
5.80	8.8 ± 1.7	12 ± 7	10.4 ± 1.6
6.50	3.2 ± 0.3	7 ± 2	5.1 ± 1.9
7.00	1.3 ± 0.4	1.1 ± 0.3	1.19 ± 0.11
7.50	0.54 ± 0.14	0.89 ± 0.17	0.72 ± 0.18
8.00	0.21 ± 0.07	0.47 ± 0.16	0.34 ± 0.13

[a] 25 °C, [Pt(II)] = 1.90×10^{-4} M, $[d(T_8p(S)T_8)] = 9.6 \times 10^{-6}$ M, $[P_i] = 5.00 \times 10^{-2}$ M.

Table 4. Results Obtained by Fitting the Experimental Data for the Reaction of $d(T_np(S)T_n)$ with *cis*-$[Pt(NH_3)(NH_2C_6H_{11})Cl_2]$ to the Mechanism Defined by Eqs 3, 7, and 8[a]

10^3[Pt(II)], M	10^4[oligo], M	k_{ah}, s^{-1}	k_2, M^{-1} s^{-1}
		Reaction with d(Tp(S)T)	
0.226	0.47	2.00×10^{-5}	fixed: 0.182[b]
0.958	0.47	2.05×10^{-5}	
1.90	0.50	3.88×10^{-5}	
		av: $(2.64 \pm 1.07) \times 10^{-5}$	
		Reaction with $d(T_8p(S)T_8)$	
0.0476	0.11	9.37×10^{-6}	fixed: 7.05[b]
0.238	0.11	9.61×10^{-6}	
0.476	0.11	1.89×10^{-5}	
		av: $(1.26 \pm 0.54) \times 10^{-5}$	

[a] 25 °C, pH 6.50, $[Na^+] = 0.064$ M. [b] The second-order rate constant for the adduct formation step was fixed to the extrapolated second-order rate constant in acidic solution by using eq 6 and $K_a = 4.1 \times 10^{-7}$ M^{-1}.

whereas that for consumption of d(Tp(S)T) was ca. 90 min (Figure S8 (Supporting Information)).

Discussion

Identification of Products. The introduction of phosphorothioate groups into both DNA and RNA results in preferential metalation of these sites by soft metal ions.[39,41-43] In a preliminary communication we reported that this preference is partially a consequence of kinetic factors, with a 3-fold higher reactivity between **2a** and the phosphorothioate moiety compared to the d(GpG) sequence.[24] Inspection of the HPLC traces in Figure 2 reveals that the two unplatinated diastereomers of d(Tp(S)T) have similar reactivities. Addition of the platination reagent led to complete conversion to products within ca. 1.5 h under the present experimental conditions. The charge neutralization reaction between **2a** and d(Tp(S)T) affords species with longer retention time than those of either reactant, and the two platinated R_p and S_p diastereomers elute as a single peak with a retention time of ca. 39 min. In the case of the longer oligonucleotides, orientational isomers of each diastereomer might be expected,[37,38] and the corresponding slow-moving peak had features that clearly revealed several components (Figures S3 and S4 (Supporting Information)). Disappearance of unplatinated oligonucleotides is followed by redistribution of products as revealed, for example, by the last HPLC traces in Figure 2. The time frame for this reaction fits well with that expected for hydrolysis of the second Cl^- ligand on the Pt complex.[27,28,52] Thus, a mixture of platinum adducts with H_2O, or OH^-, in the coordination sphere,[50] and possibly also bifunctional ones, accounts for the presence of multiple product peaks in the HPLC chromatograms obtained at longer reaction times.

Regiospecific platination of the phosphorothioate position was confirmed by ^{31}P and ^{195}Pt NMR spectroscopy, Table 1. The chemical shifts obtained by ^{31}P-NMR for the various Pt adducts, $32 < \delta < 39$ ppm, agree well with previous determinations of Pt–phosphorothioate adducts.[53] Coordination of the monofunctional $\{Pt(terpy)\}^{2+}$ moiety to d(Tp(S)T) results in two separate resonances, one for each diastereomer, in both ^{31}P- and ^{195}Pt-NMR, Figure 1.

Intermediates in the Reaction of *cis*-$[Pt(NH_3)(NH_2C_6H_{11})Cl_2]$ with Phosphorothioates. Formation of a reactive, cationic aqua complex is a crucial step in the reaction mechanism for binding of Pt(II) complexes to DNA.[8,21,26,27] Kinetic investigations of reactions between short DNA fragments and square-planar complexes of both Pt(II) and Pd(II) have revealed that adduct formation occurs via this solvent-assisted pathway.[28,48,54] The rate of adduct formation is strongly pH dependent around physiological pH owing to the weakly acidic properties of the aquated platinum complex. The pK_a values for cisplatin and related complexes normally fall in the range 6–7.[55] The decrease in reactivity, normally 1–2 orders of magnitude, with increasing pH in the range 5–8 is a further indication of the participation of the monoaqua complex as a crucial intermediate in adduct formation and of the inefficiency of the direct substitution pathway.

The previously reported[24] kinetic preference for phosphorothioate adduct formation rather than monofunctional binding

(52) Miller, S. E.; House, D. A. *Inorg. Chim. Acta* **1989**, *166*, 189–197.
(53) Slavin, L. L.; Cox, E. H.; Bose, R. N. *Bioconjugate Chem.* **1994**, *5*, 316–320.
(54) Suvachittanout, S.; Hohmann, H.; van Eldik, R.; Reedijk, J. *Inorg. Chem.* **1993**, *32*, 4544–4548.
(55) Howe-Grant, M. E.; Lippard, S. J. In *Metal Ions in Biological System*; Sigel H., Ed.; Marcel Dekker: New York, 1980; Vol. 11, pp 63–125.

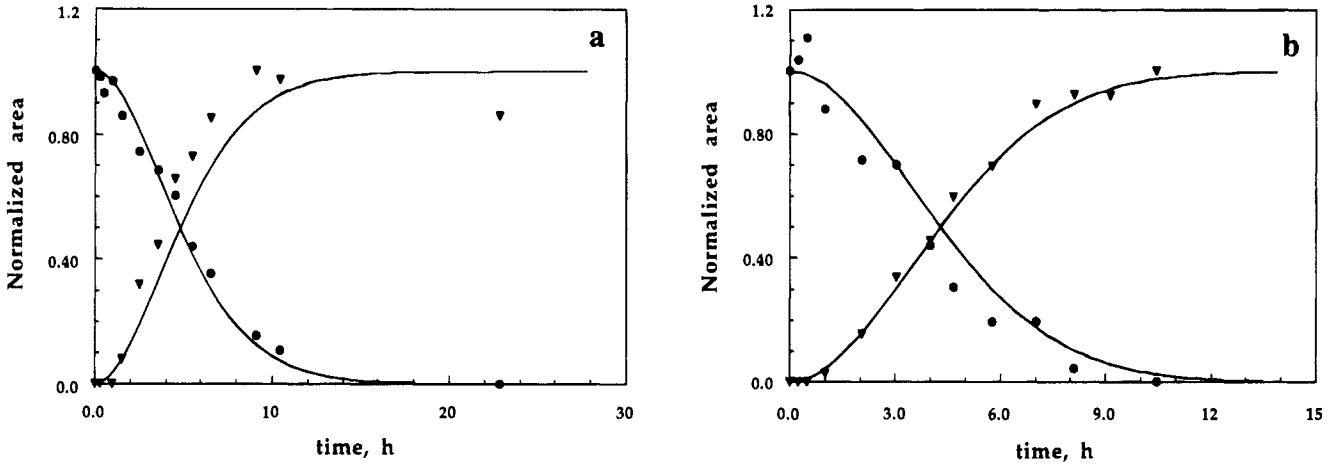

Figure 6. Experimental data points and best theoretical fits to the mechanism defined by eqs 3, 7, and 8 for reaction of **1** with (a) d(Tp(S)T), [Pt(II)] = 1.90 × 10^{-3} M, [d(Tp(S)T)] = 5.0 × 10^{-5} M, and (b) d(T_8p(S)T_8), [Pt(II)] = 2.34 × 10^{-4} M, [d(T_8p(S)T_8)] = 1.1 × 10^{-5} M. The normalized area of the unplatinated oligonucleotide is denoted by circles, and the growth of the area of platinated products, by triangles. The theoretical fits are shown as solid lines.

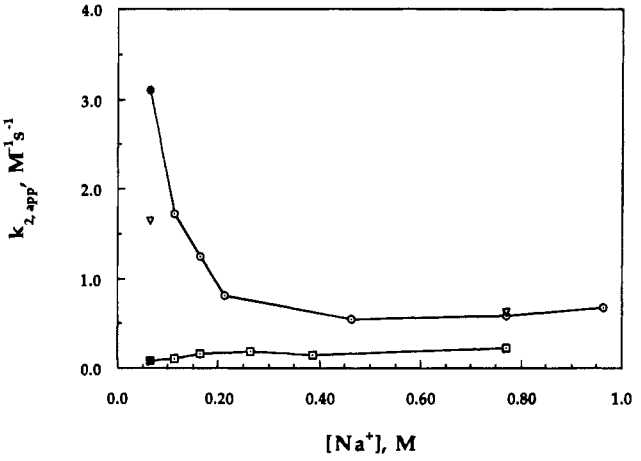

Figure 7. Sodium ion dependence for the reactions of **2a** with d(T_8p(S)T_8) (circles), d(T_4p(S)T_4) (triangles), and d(Tp(S)T) (squares), at pH 6.50 and 25 °C. Experimental information is given in Table 2 and S2 (Supporting Information). Closed symbols refer to second-order rate constants reported elsewhere.[24]

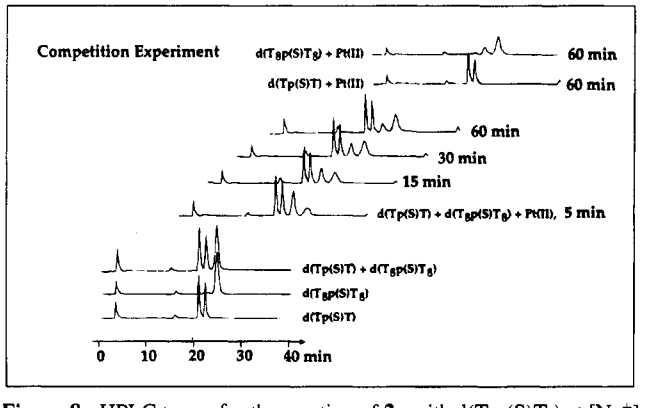

Figure 8. HPLC traces for the reaction of **2a** with d(T_8p(S)T_8) at [Na^+] = 0.064 M and pH 6.50 in the presence of d(Tp(S)T) as competing reagent and the following concentrations: [Pt(II)] = 3.41 × 10^{-4} M, [d(Tp(S)T)] = 9.54 × 10^{-5} M, and [d(T_8p(S)T_8] = 9.58 × 10^{-6} M.

to the d(GpG) sequence is in accord with the expected increased efficacy of the sulfur donor as entering ligand.[56,57] This property has the potential to change the reaction mechanism from one dominated by solvent assistance to one involving direct substitution. Under the present reaction conditions, however, both the pH dependence and the observed induction period in the reaction of **1** with d(Tp(S)T) and d(T_8p(S)T_8) (see Table 3 and Figure 6) strongly favor a reaction mechanism involving the monoaqua complex as the reactive intermediate. The pK_a of 6.4 ± 0.2 for **2a**, determined from the pH dependence of the reaction of **2a** with d(T_8p(S)T_8), is close to similar values observed for other monoaquated platinum complexes.[55] For example, a recent ^{15}N-NMR investigation reported a pK_a value for *cis*-[Pt(NH_3)$_2$Cl(OH_2)]$^+$ of 6.41.[50] The averaged rate for acid hydrolysis of **2a**, k_{ah} = (1.9 ± 0.7) × 10^{-5} s^{-1}, determined from reactions with d(Tp(S)T) and d(T_8p(S)T_8) (Table 4), is in good agreement with previous determinations of the rate of acid hydrolysis of related compounds in both the presence and the absence of trapping reagents.[27,28,58]

Mechanistic Considerations of the Differences in Reactivity among d(Tp(S)T), d(T_4p(S)T_4), and d(T_8p(S)T_8). Interactions between extended DNA and cations have been successfully described both by the counterion condensation (CC) theory and by Poisson−Boltzmann (PB) and Monte Carlo (MC) methods. Qualitatively, all methods predict the same phenomenon, namely, that of condensation of cations on the surface of a polyanion with a charge density greater than 1. A plausible explanation for the higher reactivity exhibited by the longer oligonucleotides in the present study would be to regard it as the result of an increased local concentration of the Pt complex on the polymer. We consider two mechanistic models, one purely electrostatic (model A) and the other combining electrostatic and surface effects (model B).

In model A, **2a** accumulates on the polymer such that eq 2 can be rewritten as indicated by eq 9. This equation can be used

$$k_{obsd} = k_{2,app}[Pt(II)]_{loc} \quad (9)$$

to estimate directly [Pt(II)]$_{loc}$. In the purely electrostatic case, such accumulation will parallel that of other monovalent cations, preserving the bulk ratio between these cations.[14,15] Rate variations may therefore be used indirectly to estimate the total local concentrations of cations on the polymer, provided that nonreacting cations are present in large excess over **2a**. The 40-fold higher rate constant determined for d(T_8p(S)T_8) compared to d(Tp(S)T) ([Na^+] = 0.064 M) translates to local concentration of sodium ions on the polymer of [Na^+]$_{loc}$ = 2.5

(56) Peloso, A. *Coord. Chem. Rev.* **1973**, *10*, 123−181.
(57) Elmroth, S.; Bugarcic, Z.; Elding, L. I. *Inorg. Chem.* **1992**, *31*, 3551−3554.
(58) Miller, S. E.; House, D. A. *Inorg. Chem. Acta* **1989**, *161*, 131−137.

Table 5. Comparison of the Experimentally Obtained and Calculated Estimates of Local Cation Concentration on Short Single-Stranded (ss) and Double-Stranded (ds) Oligonucleotides

Experimental Observations

oligonucleotide	$[Na^+]$, M	$k_{2,app}$, M^{-1} s^{-1}	$C_{+,loc}$ M[a] model A	$C_{+,loc}$ M[a] model B
ss d(Tp(S)T), $\|Z\| = 1$	0.064	0.080	0.064	0.064
ss $d(T_4p(S)T_4)$, $\|Z\| = 7$	0.064	1.64	1.30[b]	0.18[b]
ss $d(T_8p(S)T_8)$, $\|Z\| = 15$	0.064	3.1	2.5[b]	0.35[b]

Calculations

oligonucleotide	$[Na^+]$, M	$C_{+,loc}$, M[a] polyelectrolyte model
ds DNA, $\|Z\| = 8$	0.00176	0.061[c]
ds DNA, $\|Z\| = 16$	0.00176	0.34[c]
ds DNA, $\|Z\| = 38$	0.045	1.50[d]
ds DNA, $\|Z\| = 38$	0.095	1.7[d]
ds DNA, $\|Z\| \geq 40$	0.00176	$\geq$1.13[c]
ds DNA, $\|Z\| = 320$	0.0475	2.0[d]
ds DNA, $\|Z\| = \infty$	0.00176	1.86[c]
ds DNA, $\|Z\| = \infty$	$C_{+,loc} \rightarrow 0$	1.32[e]
ss DNA, $\|Z\| = \infty$	$C_{+,loc} \rightarrow 0$	0.23[e]

[a] Local average concentrations are considered for simplicity rather than concentration at the middle position. [b] This work. [c] Reference 59. [d] Reference 16. [e] Reference 14.

M. The rate constant determined for $d(T_4p(S)T_4)$ may in a similar fashion be used to calculate $[Na^+]_{loc}$ = 1.3 M on this intermediate-length oligonucleotide (Table 5).

Local concentrations in the range 1−3 M are reasonable values for accumulation of monovalent cations on extended DNA. For example, MC calculations predict a local average concentration in the range 1.8−2.0 M for duplex DNA with more than 20 base pairs (net charge of backbone, $|Z|$, $\geq$40),[59] and values up to 3 M have been calculated for the vicinity of the phosphodiester linkage.[60] Recent work from independent groups reveals, however, that the ability of DNA to accumulate cations is diminished substantially as a function of decreasing DNA length.[16,59,61,62] A comparison of available results computed for short, double-stranded DNAs at $[Na^+]$ = 1.76 mM[59] reveals the magnitude of this effect (Table 5). These calculated results, obtained for Na^+ concentrations different from what we used and for double- rather than single-stranded DNA, need to be corrected in order to apply to the present systems. Quantitative information about how to make such corrections is not available. The 10-fold discrepancy between our estimated values for cation condensation and those obtained theoretically suggests, however, that the purely electrostatic model cannot explain our results without requiring short, single-stranded DNA oligomers to behave as extended polyanions. We consider such behavior to be most unlikely. This conclusion is supported by the similar rate constants obtained by us for both single- and double-stranded DNA, Figure 4, which disagree with theoretical expectations of cation-binding fractions for such polymers.[14,16]

The influence of electrostatics on the reactivity can also be evaluated experimentally by varying the bulk concentration of sodium ions. If, for example, bulk $[Na^+]$ exceeds the value that can be obtained in the condensation layer, then no net accumulation should occur on the polymer. The observed reactivity under such conditions will represent the inherent reactivity of the binding site. As can be seen in Figure 7, an increase of bulk $[Na^+]$ significantly reduced the rate constants for the two longer DNA fragments, $d(T_4p(S)T_4)$ and $d(T_8p(S)T_8)$. This result was not obtained with the reference system, d(Tp(S)T), which exhibited only a slightly increased rate constant in the same interval. The similar reactivities observed for $d(T_4p(S)T_4)$ and $d(T_8p(S)T_8)$ at high ionic $[Na^+]$, both greater than that of d(Tp(S)T), indicate that a contribution independent of electrostatics has been unmasked.

The combination of both surface and electrostatic contributions to reactivity, model B, provides an alternative explanation of the present results. Surface effects in reactions between metal ions and DNA have been extensively investigated.[3,63−70] Studies related to the present work, which suggest their importance for metalation of DNA by monovalent or neutral platinum complexes, include the finding that *cis*-$\{Pt(NH_3)(NH_2C_6H_{11})\}^{2+}$ forms unequal amounts of orientational isomers on DNA[37,38] and the suggested preassociation of complexes such as diaqua(1,2-diphenylethylenediamine)platinum(II) on DNA prior to covalent adduct formation with the duplex.[19] Weak van der Waals and/or H-bonding interactions with the leaving H_2O ligand, for example, may help stabilize the transition state for substitution, thereby lowering the activation energy. If we take as the reference rate in model B the inherent reactivity represented by the common rate constant for $d(T_4p(S)T_4)$ and $d(T_8p(S)T_8)$, $k_{2,app} \approx 0.6$ M^{-1} s^{-1} at $[Na^+]$ = 0.772 M, the electrostatic component can be visualized by the increasing rate constants observed at decreasing $[Na^+]$, Figure 7. At the lowest sodium ion concentration investigated, $[Na^+]$ = 0.064 M, this increase is a factor of ca. 2.8 for $d(T_4p(S)T_4)$ and 5.6 for $d(T_8p(S)T_8)$. The resulting estimates for $[Na^+]_{loc}$ on these polymers are 0.18 and 0.35 M, respectively, now in relatively good agreement with theoretically obtained values (Table 5).

The mechanism corresponding to model B is best described by adding two elementary steps to the acid−base equilibrium in eq 3. Reversible, diffusion-controlled preassociation first occurs at the DNA surface interaction site (DNA_{si}, eq 10)

$$\mathbf{2a} + DNA_{si} \underset{k_{-1}}{\overset{k_1}{\rightleftharpoons}} \mathbf{2a}\cdot\cdot\cdot DNA_{si} \qquad (10)$$

$$\mathbf{2a}\cdot\cdot\cdot DNA_{si} + DNA_S \xrightarrow{k_2'} \mathbf{2a}\text{-}DNA_S + DNA_{si} \qquad (11)$$

followed by rate-determining adduct formation with the sulfur donor in the phosphorothioate linkage, eq 11 (see also Scheme 1). Application of the usual steady-state assumption to the surface-bound intermediate [$\mathbf{2a}\cdot\cdot\cdot DNA_{si}$] gives rise to the rate law for disappearance of the unplatinated oligonucleotide in eq 12. The use of pseudo-first-order conditions, with Pt(II) in excess, allows for simplification of eq 12 to eq 13, under the

(59) Olmsted, M. C.; Anderson, C. F.; Record, M. T. *Proc. Natl. Acad. Sci. U.S.A.* **1989**, *86*, 7766−7770.
(60) Conrad, J.; Troll, M.; Zimm, B. H. *Biopolymers* **1988**, *27*, 1711−1732.
(61) Fenley, M. O.; Manning, G. S.; Olson, W. K. *Biopolymers* **1990**, *30*, 1191−1203.
(62) Stein, V. M.; Bond, J. P.; Capp, M. W.; Anderson, C. F.; Record, M. T. *Biophys. J.*, in press.
(63) Krotz, A. H.; Hudson, B. P.; Barton, J. K. *J. Am. Chem. Soc.* **1993**, *115*, 12577−12578.
(64) Krotz, A. H.; Kuo, L. Y.; Shields, T. P.; Barton, J. K. *J. Am. Chem. Soc.* **1993**, *115*, 3877−3882.
(65) Xu, Q.; Jampani, S. R. B.; Braunlin, W. H. *Biochemistry* **1993**, *32*, 11754−11760.
(66) Black, C. B.; Cowan, J. A. *J. Am. Chem. Soc.* **1994**, *116*, 1174−1178.
(67) Buckin, V. A.; Kankiya, B. I.; Rentzeperis, D.; Marky, L. A. *J. Am. Chem. Soc.* **1994**, 9423−9429.
(68) Kalsbeck, W. A.; Thorp, H. H. *Inorg. Chem.* **1994**, *33*, 3427−3429.
(69) Sitlani, A.; Barton, J. K. *Biochemistry* **1994**, *33*, 12100−12108.
(70) Watt, T. A.; Collins, J. G.; Arnold, A. P. *Inorg. Chem.* **1994**, *33*, 609−610.

Scheme 1

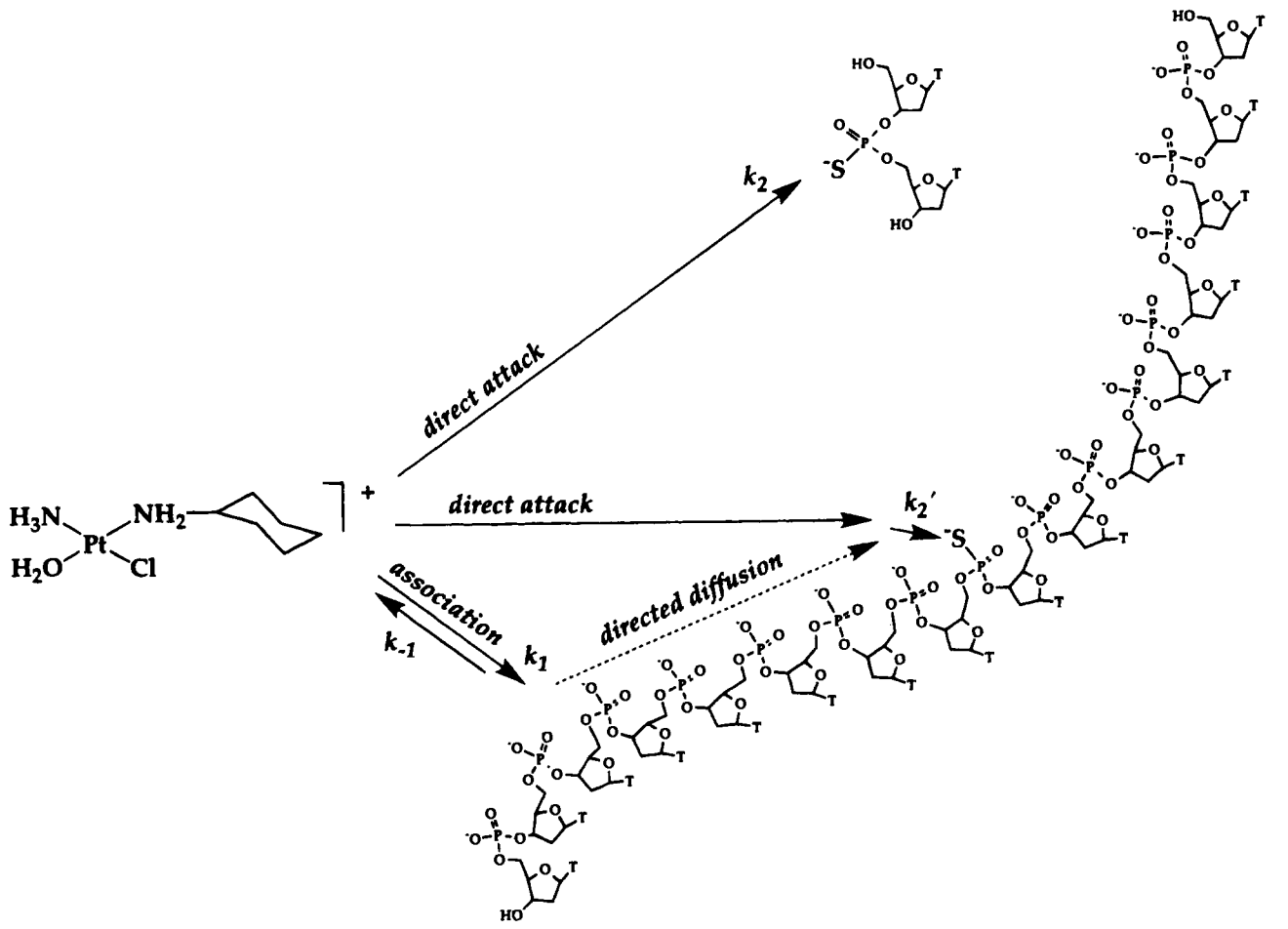

$$\frac{d[prod]}{dt} = \frac{-d[DNA_S]}{dt} = k_2' \frac{k_1[\mathbf{2a}][DNA_{si}][DNA_S]}{k_{-1} + k_2'[DNA_S]} \quad (12)$$

$$\frac{d[prod]}{dt} = \frac{-d[DNA_S]}{dt} = k_2' K_1[\mathbf{2a}][DNA_{si}][DNA_S] \quad (13)$$

assumption that the contribution from the product, $k_2'[DNA_S]$, is negligible in comparison with the rate of dissociation of **2a** from DNA. The expression for the observed pseudo-first-order rate constant, k_{obsd}, is given in eq 14, and that for the apparent second-order rate constant in eq 15. Inspection of eq 15 reveals

$$k_{obsd} = k_2' K_1[\mathbf{2a}][DNA_{si}] \quad (14)$$

$$k_{2,app} = k_2' K_1 \frac{[H^+]}{[H^+] + K_a}[DNA_{si}] \quad (15)$$

that the apparent second-order rate constant, $k_{2,app}$, is directly proportional to the concentration of preassociation sites on the DNA, $[DNA_{si}]$. This prediction fits well with our observed 2-fold difference of the apparent second-order rate constants obtained for $d(T_8p(S)T_8)$ and $d(T_4p(S)T_4)$ at $[Na^+] = 0.064$ M. The similar reactivities obtained in the present study for single- and double-stranded oligonucleotides reveal, however, that, despite the qualitative success of the simplified mechanism outlined above, additional refinements are needed to account for all of the experimental results.

To our knowledge, the data presented here are the first reported that clearly reveal contributions from both electrostatics and surface interactions to the observed reactivity for reactions involving covalent adduct formation between small inorganic molecules and DNA. The mechanistic model suggesting directed diffusion along the DNA as a significant contribution to the reactivity is similar to one proposed for DNA length-dependent diffusion-controlled association of the *lac* repressor with its operator sequence.[71-74] Its extension to small molecule–DNA interactions should be considered in both mechanistic studies and rational drug design.

Conclusions. The present work suggests that preassociation equilibria may have a significant influence on the rate of metal binding to DNA. The principal mechanistic difference between the properties of the reference system, d(Tp(S)T), and those of the extended macromolecules is illustrated in Scheme 1. The reactivity of the small reference system containing the specific binding site alone affords an estimate of the efficacy of the direct substitution reaction. Lengthening the oligomer adds closely connected and rapidly interchanging preassociation sites which direct and restrict the diffusion of associated cations along the polymer surface. As long as such directed diffusion is rapid compared to adduct formation, this association will increase the observed reactivity by increasing the probability of collisions between reactants. The apparent rate of adduct formation will consist of two components, one from the direct reaction and one from molecules already associated with the DNA. The relative contributions to the two are determined both by the

(71) Berg, O. G.; Winter, R. B.; von Hippel, P. H. *Biochemistry* **1981**, *20*, 6929–6948.
(72) Winter, R. B.; Berg, O. G.; von Hippel, P. H. *Biochemistry* **1981**, *20*, 6961–6977.
(73) von Hippel, P. H.; Berg, O. G. *J. Biol. Chem.* **1989**, *264*, 675–678.
(74) Khoury, A. M.; Lee, H. J.; Lillis, M.; Lu, P. *Biochem. Biophys. Acta* **1990**, *1087*, 55–60.

magnitude of the preassociation constant and by the number of connected pre-equilibrium sites. A challenge for future work will be to take advantage of these effects to increase the efficacy and selectivity of DNA reagents that covalently modify DNA.

Acknowledgment. This work was supported by U.S. Public Health Service Grant CA 34992 from the National Cancer Institute and a research grant from the Swedish Cancer Foundation (940140).

Supporting Information Available: Tables S1 and S2, listing experimental conditions and observed rate constants for the reaction of **2a** with DNA as a function of excess reagent and sodium ion concentration and Figure S1 showing the melting profile of dA_{16}•$d(T_8p(S)T_8)$, Figure S2, showing ^{31}P NMR spectra, Figures S3 and S4, giving representative examples of HPLC traces for reactions with $d(T_4p(S)T_4)$ and $d(T_8p(S)T_8)$, Figure S5, reporting apparent second-order rate constants as a function of oligonucleotide length, Figure S6, illustrating the pH dependent reactivity of **2a** with $d(T_8p(S)T_8)$, Figure S7, comparing HPLC traces for reaction on ss and ds DNA, and Figure S8, showing a competition experiment with $[Na^+] = 0.708$ M (17 pages). Ordering information is given on any current masthead page.

IC9502382